Cancer Chemother Pharmacol (2010) 65:877–888
DOI 10.1007/s00280-009-1093-7

ORIGINAL ARTICLE

Induction of necrosis and cell cycle arrest in murine cancer cell lines by *Melaleuca alternifolia* (tea tree) oil and terpinen-4-ol

S. J. Greay · D. J. Ireland · H. T. Kissick · A. Levy · M. W. Beilharz · T. V. Riley · C. F. Carson

Received: 5 May 2009 / Accepted: 21 July 2009 / Published online: 13 August 2009

Abstract
Purpose To examine the in vitro anticancer activity of *Melaleuca alternifolia* (tea tree) oil (TTO), and its major active terpene component, terpinen-4-ol, against two aggressive murine tumour cell lines, AE17 mesothelioma and B16 melanoma.
Methods Effects of TTO and terpinen-4-ol on the cellular viability of two tumour cell lines and fibroblast cells were assessed by MTT assay. Induction of apoptotic and necrotic cell death was visualised by fluorescent microscopy and quantified by flow cytometry. Tumour cell ultrastructural changes were examined by transmission electron microscopy and changes in cell cycle distribution were assessed by flow cytometry, with changes in cellular morphology monitored by video time lapse microscopy.
Results TTO and terpinen-4-ol significantly inhibited the growth of two murine tumour cell lines in a dose- and time-dependent manner. Interestingly, cytotoxic doses of TTO and terpinen-4-ol were significantly less efficacious against non-tumour fibroblast cells. TTO and terpinen-4-ol induced necrotic cell death coupled with low level apoptotic cell death in both tumour cell lines. This primary necrosis was clarified by video time lapse microscopy and also by transmission electron microscopy which revealed ultrastructural features including cell and organelle swelling following treatment with TTO. In addition, both TTO and terpinen-4-ol induced their inhibitory effect by eliciting G1 cell cycle arrest.
Conclusion TTO and terpinen-4-ol had significant anti-proliferative activity against two tumour cell lines. Moreover, the identification of primary necrotic cell death and cell cycle arrest of the aggressive tumour cells highlights the potential anticancer activity of TTO and terpinen-4-ol.

Keywords Tea tree oil · Terpenes · Necrosis · Apoptosis · Cell cycle arrest · Anticancer

Electronic supplementary material The online version of this article (doi:10.1007/s00280-009-1093-7) contains supplementary material, which is available to authorized users.

S. J. Greay (✉) · D. J. Ireland · H. T. Kissick · M. W. Beilharz · T. V. Riley · C. F. Carson
Discipline of Microbiology and Immunology (M502), School of Biomedical, Biomolecular and Chemical Sciences, The University of Western Australia, 35 Stirling Highway, Crawley, WA 6009, Australia
e-mail: srooney@cyllene.uwa.edu.au

A. Levy · T. V. Riley
Division of Microbiology and Infectious Diseases, PathWest Laboratory Medicine WA, Queen Elizabeth II Medical Centre, Nedlands, WA 6009, Australia

Introduction

Monoterpenes, secondary plant metabolites which consist of two isoprene units, are largely non-nutritive, give essential oils their distinctive odour and are mainly involved in plant defences (reviewed in [1–3]). Numerous terpenes have been successfully used as anticancer agents. These include vinblastine and vincristine, and paclitaxel, the most widely used chemotherapeutic agent in the treatment of breast, ovarian and lung cancer (reviewed in [4]).

Perillyl alcohol (POH), a monoterpene found in plants including sage, lemongrass, and cherries, has demonstrated anticancer activity involving Ras suppression. It induces apoptosis and G1 cell cycle arrest in numerous tumour cell lines in vitro [5, 6], and demonstrates significant in vivo antitumour efficacy [7–9]. A topical formulation is currently in phase II clinical trials for the treatment of actinic keratoses (precancerous lesions) and recently published phase I/II

studies of POH have shown that intra-nasal treatment (by inhalation) stabilises recurrent gliomas and even regresses these aggressive inaccessible tumours in some human patients [10, 11]. Ingenol-3-angelate (also known as ingenol mebutate and PEP005), a diterpene isolated from the sap of *Euphorbia peplus*, has demonstrated similar topical anticancer activity against subcutaneous melanoma tumours in mice [12]. Its mode of action involves primary cell death by necrosis [12], activation of protein kinase C [13], the activation of neutrophils [14], and the induction of G1 and G2/M cell cycle arrest [15]. More recently, in a phase IIa clinical trial Siller et al. [16] demonstrated that a topical formulation is effective for patients with actinic keratoses.

Tea tree oil (TTO), the essential oil from the Australian native *Melaleuca alternifolia* Myrtaceae, consists largely of monoterpenes and has demonstrated a variety of beneficial efficacies including antimicrobial [17], antifungal [18], antiviral [19], and anti-inflammatory activity [20]. TTO contains over 100 components, the major ones being terpinen-4-ol, γ-terpinene, α-terpinene, 1, 8-cineole and ρ-cymene. It is the most abundant component, terpinen-4-ol, that is the likely mediator of the in vitro and in vivo efficacy of TTO [21]. In vitro anticancer activity has also been identified [22, 23]. Human melanoma and adriamycin-resistant human melanoma cells treated with TTO and terpinen-4-ol underwent caspase-dependent apoptosis, a process thought to involve plasma membrane interaction via lipid reorganisation [23]. Interestingly, both TTO and terpinen-4-ol were more effective against the resistant cell line suggesting that perhaps neither are substrates for P-glycoprotein, a very useful property in the treatment of multidrug resistant tumours. Moreover, another study has demonstrated in vitro anticancer efficacy of 1,8-cineole against two human leukaemia cells lines through apoptosis [24]. However, if the high variability in response of different cancer cells following treatment with cytotoxic agents is considered, then further studies of potential anticancer agents with a variety of cell lines are necessary. Accordingly, this study examined the potential anticancer activity of TTO and its terpene components. We investigated the in vitro activity of TTO and its major components against aggressive cancer cell lines by evaluating antiproliferative efficacy by MTT assay, induction of apoptosis and necrosis by annexin-V binding, the effect on cell cycle distribution, the change in morphology by video time lapse microscopy and examination of cell ultrastructure by transmission electron microscopy.

Materials and methods

Cell culture

The AE17 murine mesothelioma cells were derived from the peritoneal cavity of C57BL/6J mice injected with asbestos fibres as previously described [25, 26]. AE17, B16-F10 murine melanoma cells and L929 murine fibroblasts were cultured in RPMI-1640 media supplemented with 10% foetal calf serum (FCS), 2 mM L-glutamine, antibiotics (50 mg/l gentamicin, 60 mg/l benzyl penicillin) and 0.05 mM 2-mercaptoethanol. HF32 human fibroblast cells (kindly supplied by PathWest Laboratory Medicine WA, Nedlands, WA) were maintained in minimum essential medium (MEM) supplemented with 10% FCS, 2 mM L-glutamine and antibiotics (5,000 units/ml penicillin and 5 mg/ml streptomycin).

TTO and components

TTO compliant with the International Standard 4730 [27] was kindly provided from P. Guinane Pty. Ltd., Chinderah, NSW. Batch 1216 was used for all studies and contained the following major components: 42.4% terpinen-4-ol; 20.1% γ-terpinene; 9.0% α-terpinene; 3.7% 1,8-cineole and 3.1% ρ-cymene as determined by gas-chromatography mass spectrometry carried out by NSW Department of Primary Industries, Diagnostic and Analytical Services, Environmental Laboratory, Wollongbar, NSW.

Terpinen-4-ol (Acros Organics, NJ.) was 97% pure, γ-terpinene and ρ-cymene (Aldrich Chemical Co. Inc., Milwaukee, WI.) were 97 and 99% pure, respectively, α-terpinene and 1, 8-cineole (Sigma Chemical Co., St Louis, MO.) were 94% and at least 99% pure, respectively. Stock solutions of these and TTO were made by dissolving 11 µl in 5.5 ml warm supplemented media with rigorous vortexing; this 0.2% solution was further diluted (0.01–0.1%) in warm supplemented media. Staurosporine, included as a positive control, was made as a stock solution of 1 mM in DMSO and stored at 4°C.

MTT 3-(4, 5-dimethylthiazol-2yl)-2, 5-diphenyltetrazolium bromide assay

To measure anti-proliferative activity (cell viability), cells (1,800/well) subcultured in 96-well plates (6 replicates) with overnight adherence, were treated with 0.01–0.15% v/v TTO, terpinen-4-ol, γ-terpinene, α-terpinene, 1,8-cineole or ρ-cymene in tissue culture media (150 µl/well) for 24–72 h. Following this, 50 µl of MTT (Sigma Chemical Co., St Louis, MO.) solution (5 mg/ml in sterile PBS) was added to each well and incubated for 3–6 h at 37°C. The solution was then gently aspirated from each well, and 160 µl of 10% sodium dodecyl sulphate (SDS in dH_20) was added, following an overnight incubation at 37°C to dissolve the formazan crystals. Absorbance was measured in a microplate reader using a filter at 570 nm. Results were expressed as a percentage of the control wells. IC_{50} (concentration

eliciting 50% inhibition) values were determined by linear and polynomial regression.

Visualisation and quantification of apoptosis and necrosis

For visualisation of apoptosis and necrosis, cells (5×10^4/1.5 ml) were grown on sterile 22 mm^2 coverslips in 6-well tissue culture dishes, with overnight incubation. Attached cells were treated with TTO, terpinen-4-ol, staurosporine or culture media (control) and incubated for 24 h. Following this, any floating cells were collected by centrifugation, and washed twice with PBS. Cells were then triple stained with Hoechst 33342 (Sigma Chemical Co., St Louis, MO.) annexin V-fluorescein isothiocyanate (FITC) (Biovision Inc., Mountain View, CA) and propidium iodide (PI) (Biovision Inc., Mountain View, CA) by resuspending cell pellets in 20 µl of 1× annexin V-FITC binding buffer (Biovision Inc., Mountain View, CA) containing 2 µl of annexin-V-FITC (0.25 mg/ml), 1 µl PI (1 mg/ml) and 1 µl of Hoechst 33342 (1 mg/ml/PBS) and added to microscope slides. Corresponding coverslips with washed attached cells were then inverted, added to the slides and stained for 15 min in the dark. Cells were analysed by fluorescence microscopy (magnification 20×, 40×) using a triple filter. The morphological appearance of apoptosis was characterised by cell rounding, membrane bleb/blister formation, nuclear condensation and fragmentation, and apoptotic body formation with the retention of membrane integrity. Apoptotic cells were identified as brightly fluorescing Hoechst 33342 stained cells displaying shrinkage with condensed, segmented nuclei with apoptotic bodies coupled with bound annexin V-FITC green staining in the plasma membrane. The morphological appearance of necrosis was characterised by cell swelling, nuclear swelling and the loss of plasma membrane integrity. These necrotic cells were identified by brightly fluorescent Hoechst stained nuclei independent of chromatin condensation, coupled with double staining of both annexin V-FITC and PI or PI alone (red staining).

Quantification of apoptosis and necrosis following treatments was carried out by flow cytometry using an annexin V-phycoerythrin (PE) apoptosis detection kit from Becton Dickson Pharmingen™ (San Diego, CA) according to the manufacturer's instructions with slight modifications. Briefly, cells (3×10^5/5 ml) cultured in 25 cm^3 tissue culture flasks with overnight adherence and treated with TTO, terpinen-4-ol, staurosporine or culture media for 24 and 48 h were harvested via trypsinisation, included with any floating cells, centrifuged and resulting pellets washed twice in ice-cold PBS (5% FCS). Cell pellets were then resuspended in 100 µl 1× Becton Dickson Pharmingen™ binding buffer containing 1 µl annexin-V-PE and 1 µl 7-amino-actinomycin (7-AAD) in FACS tubes. Cells were gently vortexed and incubated for 15 min at 25°C in the dark. Following this, 400 µl of 1× binding buffer was added to each tube which was analysed using a BD FACSCanto™ benchtop flow cytometer where annexin-V-PE positive cells were deemed apoptotic whilst 7-AAD and 7-AAD/annexin-V-PE positive cells were deemed necrotic. A minimum of 10,000 events were quantified for each treatment and analysed using FlowJo software (Treestar, Inc., San Carlos, CA) to quantify the percentage of apoptosis and necrosis in the cell populations. Comparisons were made with untreated control cells.

Video time lapse microscopy

To examine the effect of TTO on cellular morphology and to clarify necrotic cell death was not a result of secondary necrosis following apoptotic cell death, cells were cultured on glass bottom 35 mm tissue culture dishes (1.0×10^5/23 mm^2 growth area/1.5 ml) with overnight adherence and treated with 0.04% TTO or culture media. Preparations were imaged on a Nikon TiE microscope using a 20× objective, DIC imaging and a Perfect Focus System accessory. The microscope was fitted with a Tokai Hit stage top incubator INU series chamber (37°C, 5% CO_2) and images were captured every 120 s for a 24-h period on an Andor iXon EMCCD 885 camera using NIS elements AR (Nikon), commencing upon initial addition of TTO or culture medium. Images were processed using Image J software (U.S. National Institutes of Health, Bethesda, MD) and movies generated using Canopus ProCoder Express software (Canopus Corporation, San Jose, CA) using the DivX codec.

Transmission electron microscopy

The morphological appearance of apoptotic cells by transmission electron microscopy was identified by cell shrinkage, nuclear shrinkage, compaction, condensation and marginalisation of chromatin around the nuclear membrane, with membrane blebbing/blistering, nuclear fragmentation, apoptotic body formation, and mitochondrial condensation which may display fission or budding. Necrotic cells were identified by cell swelling, nuclear swelling, plasma and nuclear membrane distension and rupture, mitochondrial swelling, loss of electron density and disturbances in mitochondrial cristae. Cells cultured in 75 cm^2 tissue culture flasks (9×10^5/15 ml) with overnight adherence treated with 0.04% TTO or culture media for 24 h were harvested via trypsinisation, included with any floating cells, centrifuged and resulting pellets washed twice in ice-cold PBS. Cell pellets were fixed overnight in 1 ml of 2.5% glutaraldehyde in phosphate buffer (0.05 M, pH 7.0), then rinsed twice in buffer (1 ml, 30 min). Buffer

was removed, bovine albumin was added (0.1 ml, 10% aqueous) and pellets were gelled with the addition of 0.1 ml of fixative [28]. Gelled pellets were cut from 1.5 ml biofuge tubes and placed under fixative in small baskets for processing in a Lynx™ el Microscopy Tissue Processor. Processing involved post-fixation in osmium tetroxide (1% aqueous), dehydration in an ethanol series and embedding in propylene oxide/araldite mixtures (2× 5 min in 100% propylene oxide; 2× 30 min propylene oxide/araldite 3:1; 1× 60 min and 1× overnight 100% araldite). Samples were polymerised at 60°C, sections were cut on a LKB Bromma microtome, deposited on grids and positively stained with uranyl acetate (1% aqueous, 5 min), rinsed in sterilised distilled water (SDW), then lead citrate (2.5%, 2 min), followed by a rinse in SDW and drying over a hotplate. Excess stain was removed by rinsing in SDW and the grids were blotted dry. Samples were examined on a transmission electron microscope (Phillips CM10) fitted with MegaView III Soft Imaging System.

Analysis of cell cycle distribution

To examine the effect of treatments on cell cycle distribution, cells (3×10^5/5 ml) cultured in 25 cm^3 tissue culture flasks with overnight adherence and treated with TTO, terpinen-4-ol, staurosporine or culture media for 12, 24 and 48 h were harvested via trypsinisation, included with any floating cells, centrifuged and resulting pellets washed twice in ice-cold PBS. Cell pellets were then resuspended in 300 µl ice-cold PBS and fixed in ice-cold 70% ethanol added drop wise with vortexing following overnight incubation at 4°C. Following this, cells were centrifuged (500× *g* for 4 min) and washed once with 1 ml PBS. Cell pellets were resuspended in 500 µl of PBS containing 1 µl RNase A to give a final concentration of 200 µg/ml and incubated at 37°C for 40 min. Following incubation, 2.5 µl of PI solution (PBS) was added to give a final concentration of 10 µg/ml; cells were then vortexed and analysed by flow cytometry. A minimum of 10,000 events were quantified for each treatment. Percentages of cell cycle distribution in phases: G0/G1 (resting/gap phase 1), S (DNA synthesis phase) and G2 (gap phase 2)/M (Mitosis phase) were calculated in only (2 N (normal DNA content)/4 N (double DNA content)) gated cells by DNA content analysis using the Dean-Jett-Fox model in FlowJo software (Treestar, Inc., San Carlos, CA) and are compared with untreated, control cells.

Statistical analysis

All data are presented as mean ± standard deviation (SD). Significant differences ($P < 0.05$) between control and treated cells were conducted by Student's *t* tests.

Results

TTO and terpinen-4-ol inhibit cellular proliferation

The anti-proliferative effect of TTO and its most abundant terpene component terpinen-4-ol was examined using two murine tumour cell lines, AE17 mesothelioma and B16 melanoma. In addition, we assessed dose responses in non-tumour L929 and HF32 fibroblast cells. Cells were treated for 24 and 48 h and viability measured by the MTT assay (Fig. 1, Table 1). TTO and terpinen-4-ol had a dose-dependent effect against all cell lines tested (Fig. 1). After 24 h, both treatments were most efficacious against the AE17 cells (Fig. 1), with IC_{50} values of 0.03% for TTO, and 0.02% for terpinen-4-ol (Table 1). Increasing exposure time from 24 to 48 h significantly ($P < 0.05$) reduced TTO and terpinen-4-ol IC_{50} values against AE17 and B16 cells (Table 1); increased exposure time of both treatments to 72 h did not significantly increase the anti-proliferative effect against any cell line tested (data not shown). Doses of TTO and particularly terpinen-4-ol were considerably less efficacious against both human and murine fibroblast cell

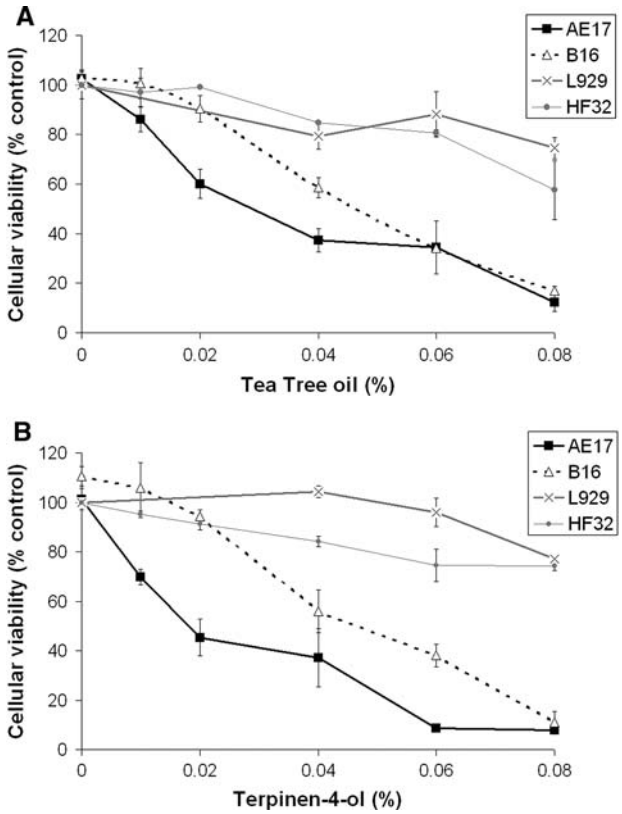

Fig. 1 Antiproliferative effect of A, TTO and B, terpinen-4-ol after 24 h against AE17 mesothelioma, B16 melanoma, L929 fibroblast and HF32 fibroblast cells. Cellular viability was assessed following treatments by the MTT proliferation assay. Results are expressed as % of control and represent the mean ± SD of at least two experiments

Table 1 IC_{50} values (%) for TTO and terpinen-4-ol after 24 and 48 h against AE17 mesothelioma, B16 melanoma and fibroblast cells, L929 and HF32

Cell lines	IC_{50} values (%)[a]			
	TTO		Terpinen-4-ol	
	24 h	48 h	24 h	48 h
AE17	0.03 ± 0.005	0.02 ± 0.006	0.02 ± 0.001	0.01 ± 0.002
B16	0.05 ± 0.007	0.03 ± 0.002	0.05 ± 0.009	0.04 ± 0.003
L929	0.1 ± 0.01	0.09 ± 0.006	N/D	0.15 ± 0.003
HF32	0.08 ± 0.01	0.07 ± 0.01	0.1 ± 0.003	0.1 ± 0.003

N/D not determined

[a] IC_{50} (%) is the amount of treatment required to inhibit cell growth by 50% compared to control cells as assessed by the MTT assay and is calculated by linear regression. Data are the mean ± SD of six replicates of at least two independent experiments

lines (Fig. 1); TTO was 2–5 fold and terpinen-4-ol was 5–15-fold less efficacious against fibroblast cells compared to AE17 and B16 tumour cells, respectively, with TTO IC_{50} values of 0.08% (24 h), 0.07% (48 h) in HF32 cells, IC_{50} values of 0.1 (24 h) and 0.09% (48 h) in L929 cells and terpinen-4-ol IC_{50} values of 0.1% in HF32 cells after both 24 and 48 h and 0.15% after 48 h in L929 cells (Table 1). Concentrations of α- and γ-terpinene, 1,8-cineole and ρ-cymene equivalent to and greater than those found in effective TTO concentrations (0.005–0.1%) had negligible efficacy against all cell lines tested (data not shown).

TTO and terpinen-4-ol induce cell death by necrosis and low level apoptosis

In order to evaluate if the anti-proliferative effect of TTO and terpinen-4-ol in tumour cells was a result of cell death, apoptosis and necrosis were evaluated following treatment. The morphological appearance of fluorescent stained AE17 and B16 cells following treatment with 0.04% TTO and terpinen-4-ol after 24 h is depicted in Fig. 2a, b. AE17 and B16 control cells had normal fluorescent Hoechst stained nuclei, with no discernable annexin-V-FITC or PI positive cells (Fig. 2a, b). In comparison, TTO and terpinen-4-ol treated AE17 cells were fewer in number, and displayed a large proportion of necrotic cells, with brightly Hoechst fluorescing nuclei, little/no nuclear condensation and in particular following TTO treatment, a large proportion of double stained annexin-V-FITC and PI positive cells, indicative of necrotic cells (Figs. 2a and 3). Treatment of B16 cells with TTO and terpinen-4-ol for 24 h reduced the cell population, with a small proportion of brightly fluorescing Hoechst stained cells and similarly small proportion of double stained annexin-V-FITC and PI positive necrotic cells.

From this morphological fluorescent analysis, the primary mode of TTO and terpinen-4-ol induced cell death in AE17 cells appeared to be necrosis. Only with concentrations of greater than 0.06% TTO and terpinen-4-ol was significant necrotic cell death evident in B16 cells (data not shown). Lower concentrations of 0.02% TTO and 0.01% terpinen-4-ol over 24–48 h did not increase apoptotic cell death in either cell line (data not shown). In order to confirm these observations and quantify levels of apoptosis and necrosis following exposure to TTO and terpinen-4-ol, flow cytometry was performed on double stained annexin-V-PE and PI cell populations (Fig. 3).

Specifically, TTO induced significant ($P < 0.05$) necrosis (36.2%) and apoptosis (13.3%) in AE17 cells after 24 h. This is consistent with the observations by fluorescent microscopy. Increased exposure time to 48 h, induced significantly ($P < 0.05$) higher levels of necrosis (55%), but apoptosis remained similar (12.7%) (Fig. 3). Conversely,

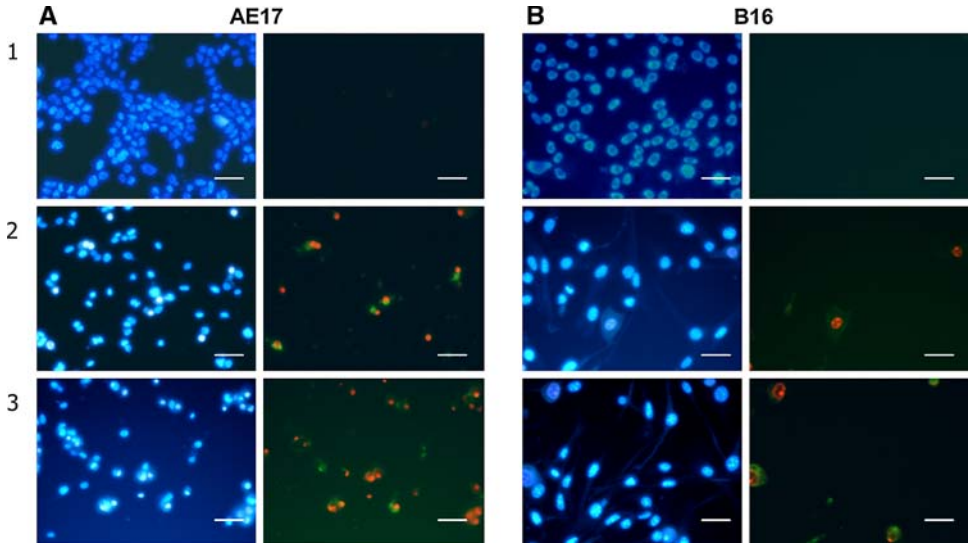

Fig. 2 Representative fluorescent microscopy images (20×, scale bar 50 µm) of **a** (AE17 mesothelioma) and **b** (B16 melanoma) of (1) control, (2) terpinen-4-ol (0.04%) and (3) TTO (0.04%) treated cells after 24 h. Brightly fluorescing Hoechst stained cells (*left*) indicate dead/dying cells and annexin-V-FITC (AV) (*green*)/propidium iodide (PI) (*red*) stained cells (right) indicate apoptotic cells (green florescence only, AV) and necrotic cells (red and green florescence AV/PI)

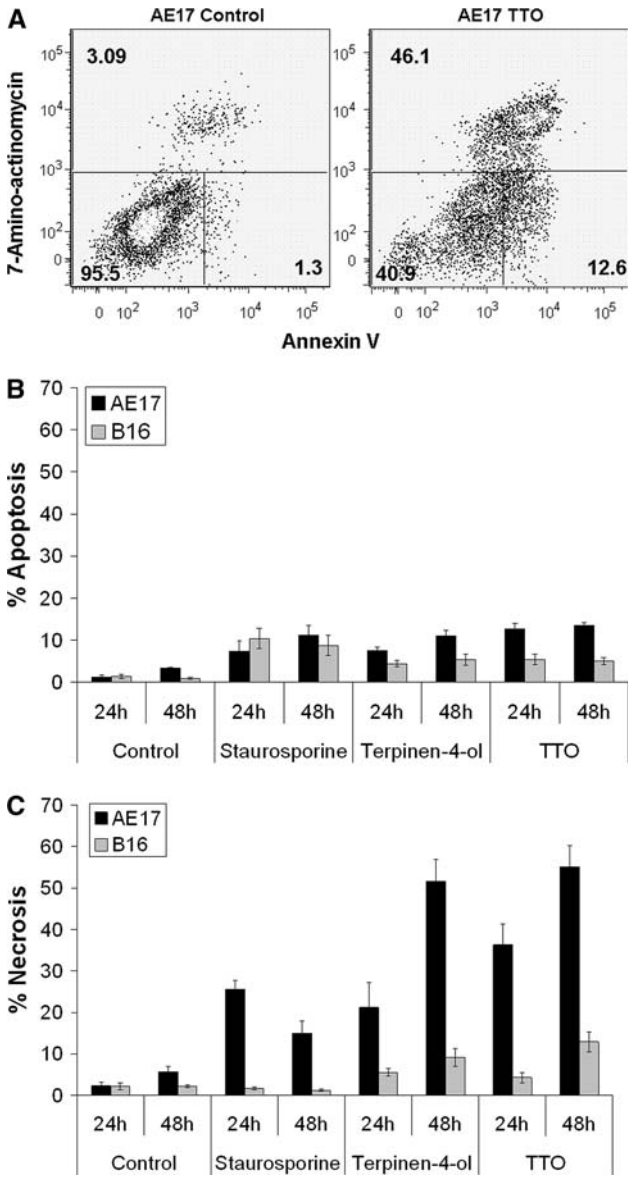

Fig. 3 Effect of terpinen-4-ol (0.04%) and TTO (0.04%) on apoptosis and necrosis of AE17 mesothelioma and B16 melanoma cells after 24 and 48 h. **a** Representative FACS plot of untreated and TTO-treated AE17 cells after 24 h. **b** % apoptosis (annexin-V-PE) and **c** % necrosis (annexin-V-PE and 7AAD) was quantified by flow cytometry using annexin V-PE and 7AAD double staining. Untreated cells served as a negative control while Staurosporine (10 nM) was included as a positive control. Data represent the mean ± SD of at least three independent experiments, quantifying a minimum of 10,000 cells per treatment

TTO induced low levels of apoptosis and necrosis at both exposure times in B16 cells; 4.3% necrosis and 5.5% apoptosis after 24 h, and 12.9% necrosis and 5.1% apoptosis after 48 h (Fig. 3b, c).

Similarly, treatment with terpinen-4-ol induced significant ($P < 0.05$) levels of both necrosis (21.2%) and apoptosis (7.5%) in AE17 cells after 24 h. Increasing the exposure time to 48 h significantly ($P < 0.05$) increased necrosis (51.6%), but apoptosis levels were again similar (11.2%) (Fig. 3b, c). As with TTO, treatment with terpinen-4-ol induced low levels of necrosis and apoptosis in B16 cells; 5.5% necrosis and 4.5% apoptosis after 24 h, and 9.1% necrosis and 5.3% apoptosis after 48 h (Fig. 3b, c).

Staurosporine, an inducer of apoptosis in numerous cell lines, included as a positive control, induced significant ($P < 0.05$) necrosis (25.6%) and low level apoptosis (7.4%) in AE17 cells after 24 h. Significant, but again low level apoptosis in B16 cells was evident after 24 h (10.5%) but with negligible necrosis, 1.6% (Fig. 3b, c). Neither increasing staurosporine exposure time to 48 h (Fig. 3b, c) nor increasing concentrations to 50–100 nM, and 1–5 μM over 6–24 h increased apoptotic cell death in either cell line (data not shown).

TTO affects AE17 and B16 cellular morphology

Video time lapse microscopy allowed the examination of morphological changes and the identification of cell death over 24 h, induced by TTO in AE17 and B16 cells compared with control untreated cells (Fig. 4a–d, Supplementary (S) movies 1–4).

AE17 control cells (Fig. 4a, S. movie 1) were extremely motile, forming blebs and protrusions to ensure cell to cell contact in order for cell division to occur. Frequent cell divisions were evident. Prior to cell division, cells detached from the substratum, rounded up, then divided and reattached. Each cell doubled in the population after approx. 19 h in culture (confirmed by cell counts, data not shown).

AE17 TTO-treated cells (Fig. 4b, S. movie 2) displayed lower levels of cell division compared to control cells between 0 and 6 h TTO treatment (S. movie 2). This was also evident by cell counts, as TTO-treated AE17 cells were ~50% fewer in number compared with control cells (data not shown). There was also evidence of an apoptotic cell, with extensive blebbing and formation of apoptotic bodies, and some primary necrotic cells evident by swelling, surface blistering and rupture following 6 h treatment. Cells appeared to divide; however, as treatment extended over 12–24 h, necrotic cells were evident (Fig. 4b, S. movie 2).

B16 control cells (Fig. 4c, S. movie 3) were also extremely motile. This movement appeared dependent on membrane protrusion and not on the formation of blebs. Cells were significantly larger than AE17 cells, with extensive cytoplasmic area and frequent cell divisions were evident. B16 cells appeared to double in approx. 16 h (confirmed by cell counts, data not shown) and appeared confluent after 24 h.

B16 TTO-treated cells (Fig. 4d, S. movie 4) displayed modest divisions compared to control cells. This was also evident by cell counts, as TTO-treated B16 cells failed to double in number compared with control cells and were in fact almost identical in number compared with the cell number at

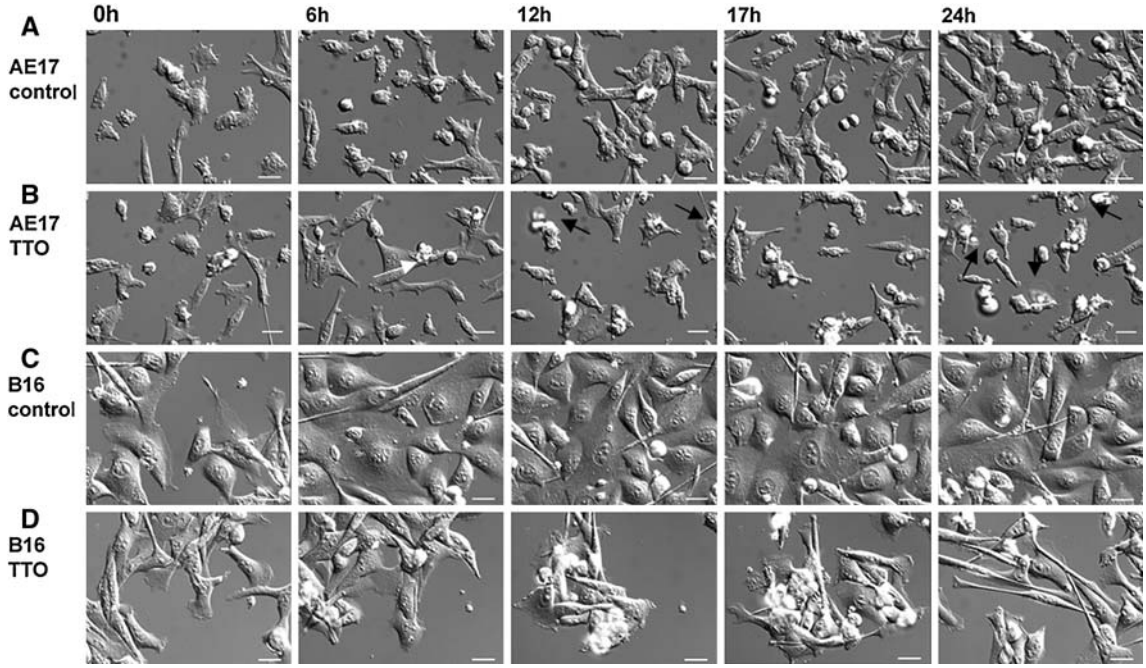

Fig. 4 Representative video time lapse microscopy DIC images (20×, scale bar 25 μm) of **a** AE17 control, **b** AE17 TTO (0.04%) treated cells, **c** B16 control and **d** B16 TTO (0.04%) treated cells after 0, 6,12,17 and 24 h. *White arrows* indicate apoptotic cells, *black arrows* indicate necrotic cells (See Supplementary material for videos S1–4)

initial treatment (data not shown). B16 cells were continuously motile and consistent with flow cytometry and fluorescent microscopy observations, displayed little cell death. Following 24 h TTO treatment, cells were elongated and had similar confluency as initial treatment at time 0 h (Fig. 4d).

TTO affects AE17 and B16 cell ultrastructure

Transmission electron microscopy allowed the examination of changes in AE17 and B16 cell ultrastructure induced by 0.04% TTO after 24 h compared with control untreated cells (Fig. 5a–d). AE17 control cells (Fig. 5a) displayed normal nuclei, a dense granulated cytoplasm, microvilli on cell surface with intact plasma membrane and nuclear envelope, healthy regions of smooth and rough endoplasmic reticulum (ER) and healthy mitochondria with parallel cristae. A large proportion of AE17 cells treated with TTO for 24 h (Fig. 5b) displayed primary necrosis characterised by nuclear swelling with a loss of electron density within the nucleus and cytoplasm; cells were abundant in ER which appeared dilated. Both the nuclear envelope and plasma membrane appeared slightly distended and disrupted. Microvilli on the cell surface had reduced in number. The appearance of some secondary lysosomes is indicative of cellular digestion of organelles, whilst rough ER appeared electron lucent and had become rounded. Mitochondria were far fewer in number compared with control cells. Those identified had become electron lucent with disturbed cristae.

B16 control cells (Fig. 5c) and the majority of B16 TTO-treated (Fig. 5d) cells both displayed similar normal nuclei with similar electron density in both the nuclei and cytoplasm. Both control and treated B16 cells were abundant with mitochondria; some TTO-treated B16 cells displayed regions of swollen golgi and cisternae of ER (Fig. 5d2), but compared with control cells, the abundance of ER was similar. B16 control cells all appeared to have intact plasma membrane with well-defined nuclear envelopes. A small proportion of TTO-treated cells had a disturbed plasma membrane and some loss of definition of the nuclear envelope (Fig. 5d3). B16 control cells had normal, healthy, electron dense mitochondria with well-defined parallel cristae. This contrasted with a small proportion of B16 TTO-treated cells that displayed electron lucent mitochondria and obvious disturbances in the cristae.

TTO and terpinen-4-ol induce cell cycle arrest

The modest apoptotic and necrotic B16 cell death following treatment, yet decreased proliferation as assessed by MTT assay, initiated the examination of the ability of TTO and terpinen-4-ol to affect the cell cycle. This was assessed in the two tumour cell lines by measuring cell cycle distribution by flow cytometry after 12, 24 and 48 h (Fig. 6). Treatment with both terpinen-4-ol and TTO significantly altered the cell cycle profile of B16 cells, with only modest changes in AE17 cells. Representative FACS plots of B16 control and TTO cells are depicted (Fig. 6a). Following

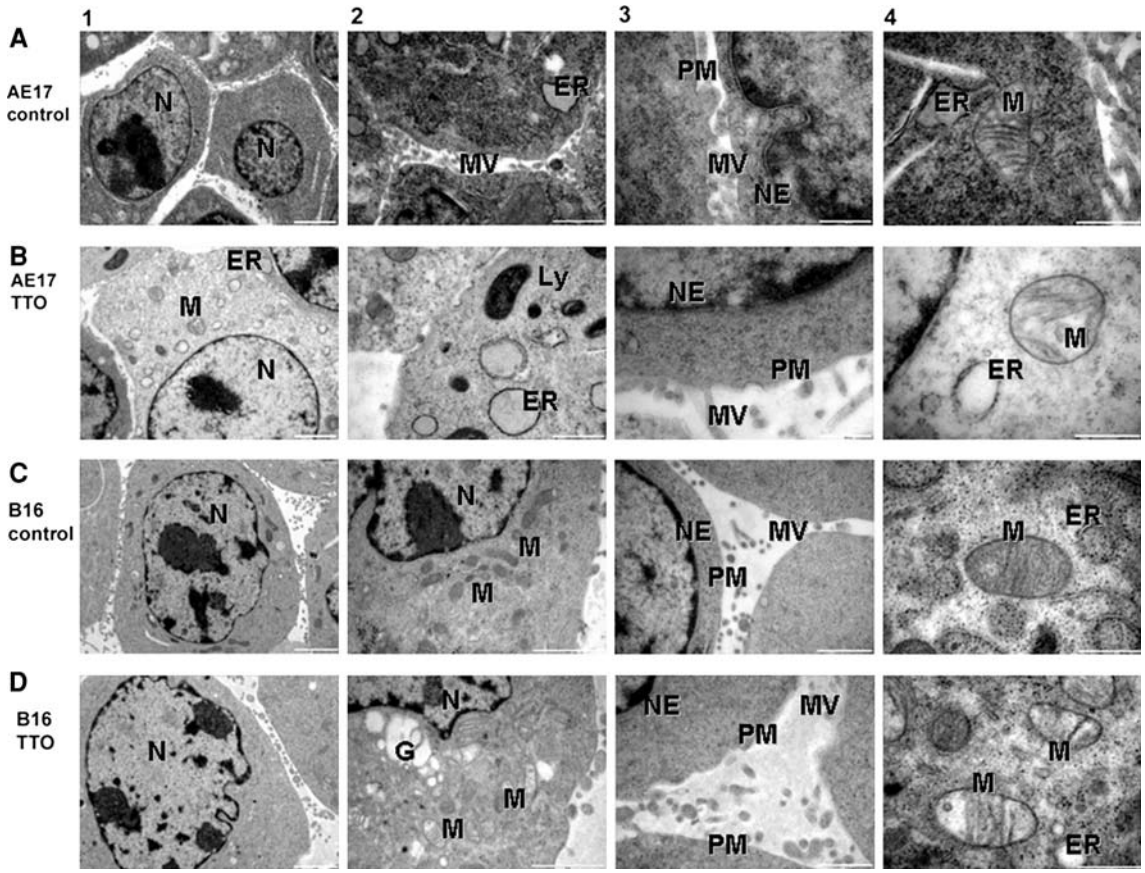

Fig. 5 Effect of TTO (0.04%) on ultrastructure of AE17 mesothelioma and B16 melanoma cells after 24 h. Representative transmission electron microscopy images: 1 (7900×, scale bar 2 μM), 2 (19,000×, scale bar 1 μM), 3 (34,000×, scale bar 500 nm), 4 (46,000×, scale bar 500 nm). **a** AE17 control cells, **b** TTO-treated AE17 cells, **c** B16 control cells, **d** B16 TTO-treated cells. *N* nucleus, *ER* endoplasmic reticulum, *M* mitochondria, *Ly* secondary lysosome, *G* golgi complex, *PM* plasma membrane, *NE* nuclear envelope, *MV* microvilli

treatment with TTO and terpinen-4-ol for 12 and 24 h, B16 cells displayed significant ($P < 0.05$) cell cycle arrest in G1 phase (Fig. 6b), a corresponding decrease in S phase (Fig. 6c) and no significant increase in G2/M phase (Fig. 6d). Increased exposure time to 48 h resulted in similar cell cycle distributions as in cells treated with TTO for 12 and 24 h. Similarly, after 24 h, staurosporine (10 nM) which induced low level apoptosis in both tumour cell lines, significantly ($P < 0.05$) induced a G1 arrest in both tumour cell lines, with a pronounced decrease in S phase and no significant decrease in G2/M phase cells (Fig. 6b–d). Increased exposure time with staurosporine to 48 h had a modest effect on B16 cells, with only a decrease in S phase (Fig. 4c), but in AE17 cells staurosporine significantly arrested cells in G1 phase and decreased cells in S phase (Fig. 6b–d).

Discussion

Previous studies have demonstrated in vitro and in vivo anticancer efficacy of terpenes such as ingenol-3-angelate [12, 15, 29], POH [5, 30–32] and D-limonene [33, 34]. Importantly, these have subsequently led to case studies and clinical trials of these agents in human patients [11, 16, 35]. Despite numerous studies demonstrating the antimicrobial efficacy of TTO and its major components (reviewed in [17]), only a single study [23] has examined anticancer activity in terms of mechanisms of action of TTO and considering the great variability in mechanisms of chemotherapeutic agents in varying cell lines; highlights the importance of this investigation.

We examined the effect of TTO and its major component terpinen-4-ol in two aggressive murine tumour cell lines, an AE17 mesothelioma and a B16 melanoma. In addition, we compared TTO and terpinen-4-ol's dose effect in murine and human fibroblast cells. TTO and terpinen-4-ol significantly inhibited the growth of the two murine tumour cell lines in a dose- and time-dependent manner as assessed by the MTT assay. This effect was more pronounced in AE17 cells than in B16 cells. TTO had a dose-dependent effect against non-tumour fibroblast cells; however, this effect was only cytotoxic at doses 2-3-fold (HF32) and 3-5-fold (L929) greater (24–48 h) compared with AE17 cells and

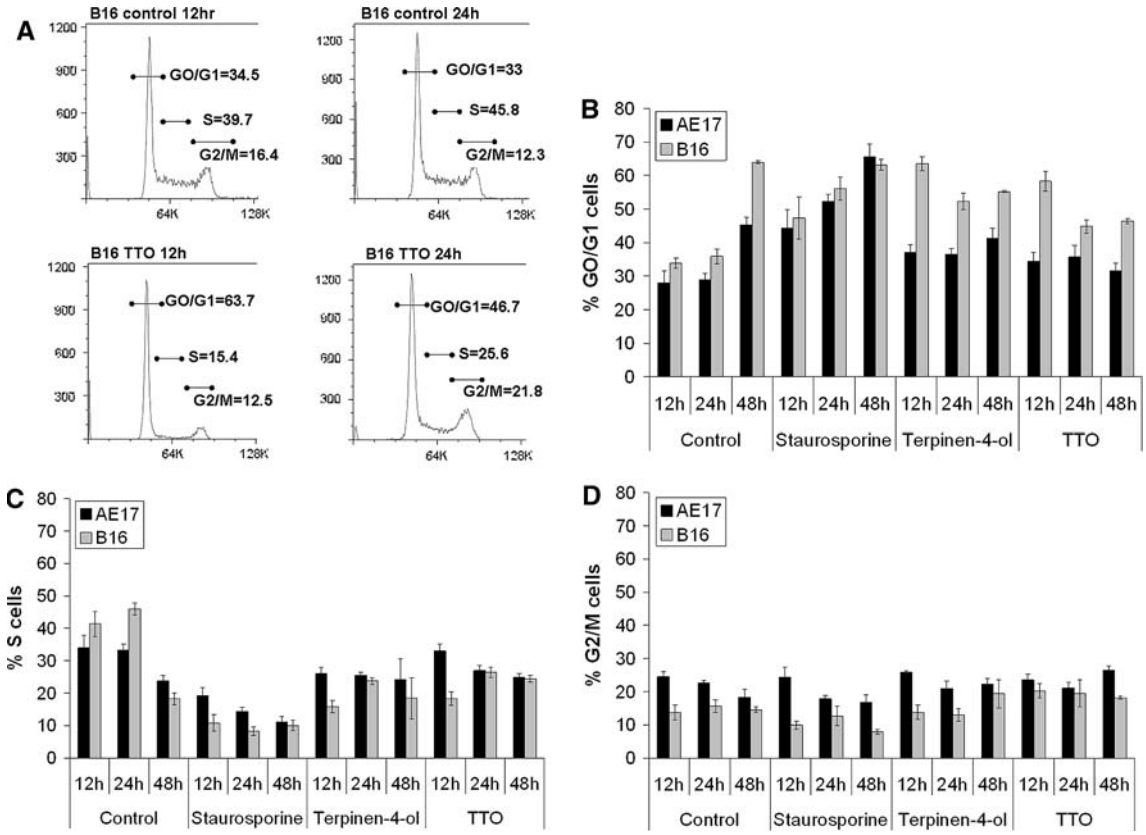

Fig. 6 Effect of terpinen-4-ol (0.04%) and TTO (0.04%) on cell cycle distribution of AE17 mesothelioma and B16 melanoma cells after 12, 24 and 48 h. **a** Representative FACS DNA profiles of propidium iodide stained untreated and TTO-treated B16 cells. Results are expressed as percentages of cell cycle distribution in phases: **b** G1, **c** S and **d** G2/M phase calculated by DNA content analysis using the Dean-Jett-Fox model in FlowJo software and are compared with control, untreated cells; staurosporine (10 nM) was included as a positive control. Data represent the mean ± SD of at least three independent experiments, quantifying a minimum of 10,000 events per treatment of only (2 N/4 N) gated cells

2-fold (HF32) and 2-3 fold (L929) greater (24–48 h) compared with B16 cells. Terpinen-4-ol was only efficacious against non-tumour fibroblasts at doses 5–10 fold (HF32) and 15-fold (L929) greater (24–48 h) than with AE17 cells and 2–3 fold (HF32) and 4-fold (L929) (24–48 h) greater compared with B16 cells. The previously reported IC_{50} value for TTO against fibroblasts after 24 h of 0.067% [36] is consistent with our current data. Moreover, non-cytotoxic doses examined in our HF32 human fibroblasts of 0.02–0.03% TTO and 0.01% terpinen-4-ol were significantly inhibitory in human M14 melanoma cells [23].

However, efficacy depends on cell types examined, as IC_{50} values reported for human cancer cell lines, HepG2 and HeLa ranged from 0.002 to 0.27% with TTO treatment [22]. Our data for AE17 cells are consistent with previously reported IC_{50} values for terpinen-4-ol against human tumour cell lines HepG2 and HeLa cell lines of 0.006–0.014% but as observed with TTO, are highly variable, depending on cell type examined. We examined the anti-proliferative activity of the other four major components of TTO, α- and γ-terpinene, 1,8-cineole and ρ-cymene, to elucidate if any contributed to the efficacy of TTO. The four components, tested at a concentration range which included equivalent doses to those found in TTO, demonstrated no significant antiproliferative activity. Only a concentration of 0.1% of ρ-cymene showed negligible efficacy against AE17 tumour cells, reducing viability by ~30% (data not shown). From these data, it appears that multiple components in TTO rather than a single active component or other components not examined here are important in terms of the in vitro antiproliferative effect. Moreover, the significant antiproliferative effect following treatment with terpinen-4-ol suggests that although it may not be solely responsible for the anti-proliferative activity of TTO, it is certainly important. The overall differential dose response to TTO or terpinen-4-ol treatment observed between tumour and non-tumour fibroblast cells in vitro suggests TTO may elicit its effect by inhibiting rapidly dividing cells more readily than slower growing non-cancerous cells, a feature of many clinical chemotherapeutic agents.

The combination of fluorescent microscopy, video time lapse microscopy, transmission electron microscopy and

flow cytometry allowed the identification and quantification of the mode of cell death induced in AE17 and B16 cells following treatment with TTO and terpinen-4-ol. AE17 cells treated with TTO and terpinen-4-ol for 24 and 48 h (0.04%) induced significant necrosis and lower levels, but significant apoptosis. Significant necrosis (~35%, data not shown) was evident only in B16 cells following an increased exposure time of 48 h and increased concentration to 0.06% TTO and terpinen-4-ol, again with negligible additional apoptosis. This correlated well with MTT assay data that indicated AE17 cells were more susceptible to TTO and terpinen-4-ol than B16 cells. Only one publication has demonstrated apoptosis induced by TTO and terpinen-4-ol in a cancer cell line. Specifically, 0.02% TTO induced ~50% apoptosis in human M14 melanoma cells following a 48 h exposure time and 0.01% terpinen-4-ol elicited over 30% apoptosis in an adriamycin-resistant M14 human melanoma cell line after 48 h. This effect was not observed in wild type M14 human melanoma cells with only ~2% apoptosis induction following the same concentration and exposure time with terpinen-4-ol [23]. Apoptosis was not the primary mode of cell death induced by TTO or terpinen-4-ol in either cell line at any other lower dose (0.005, 0.01, 0.02%), or shorter incubation time (1, 6, 12 h) (data not shown) as evident from a lack of Annexin-V positive staining independent of 7AAD or PI and in particular by video time lapse monitoring of TTO-treated cells, that identified minimal apoptosis and showed necrotic cell death was not a result of secondary apoptotic cell death. Furthermore, Hoechst staining failed to identify cells with highly condensed chromatin, fragmented nuclei or apoptotic bodies. In addition, transmission electron microscopy failed to identify cell ultrastructural features of apoptotic cell death. The absence of the classic features of apoptotic cell death including, plasma membrane blistering, chromatin aggregation and nuclear fragmentation in the TTO-treated cells analysed was apparent. The observation that TTO treatment induces changes in AE17 cells including, plasma membrane and nuclear envelope disturbance, loss of electron density within the cytoplasm, nucleus, and organelles, swelling of cell organelles and disruption of mitochondrion crista are indicative of primary necrotic cell death. The lower levels of B16 cells abundant with these ultrastructure necrotic features concur with the lower levels of necrosis observed with TTO by fluorescent microscopy and flow cytometry in this study.

The observation that TTO induced AE17 and B16 cell primary necrosis with increased concentrations and exposure times is consistent with multiple studies confirming that the antimicrobial mechanism of action of TTO involves loss of membrane integrity (reviewed in [17]). Interestingly, with the addition of staurosporine, a protein kinase inhibitor which induces apoptosis in numerous cell types, little apoptosis was observed in either AE17 or B16 cells. This could explain the low levels of apoptosis observed following treatment with TTO and terpinen-4-ol. It is not unusual to observe highly variable levels of sensitivity or varying modes of action in different cell lines. α-Hederin, a triterpene saponin found in numerous plants, induced up to 73% apoptosis in P388 murine leukaemia cells (at a concentration of 10.7 μM) [37]. At similar concentrations, α-hederin induced low level apoptosis ranging from 8 to 13% in human cancer cell lines including A549 and HEp-2 cells [38]. This variability in response may be a result of numerous factors. Both melanoma cells and mesothelioma cells are notoriously resistant to chemotherapy (reviewed in [39] and [40], respectively) and this is thought to involve apoptosis resistance. Specifically, B16-F10 cells (identical to those in this study) have mutated tumour suppressor p53 [41] and overexpress Bcl-2 [42]. These could be responsible for the apoptosis resistance and in place of apoptosis, the necrotic cell death observed in this study. Whether the mechanism of necrotic cell death observed following TTO and terpinen-4-ol treatment may involve mitochondrial damage, DNA damage, ATP depletion, and/or increased ROS production remains to be elucidated. It is possible that TTO and terpinen-4-ols interaction with plasma membrane as observed in M14 cells [23] is sufficient to mediate necrosis via loss of mitochondrial membrane potential as demonstrated with the addition of the diterpene ingenol-3-angelate to B16-F0 cells [12]. The majority of clinical chemotherapeutic agents ultimately induce tumour cell apoptosis following treatment; however, the resistance to this mode of cell death by many cancer cell lines suggests alternative targets for killing tumour cells are necessary. This is further supported by the observation that apoptosis may be reversed in cancer cells [43]. Ingenol-3-angelate induces its primary mode of cancer cell death through necrosis [12, 29], as displayed by plasma membrane and mitochondrial disruption which leads to the activation of an antitumour immune response [44]. Moreover, its success in phase IIa clinical trials against skin cancer [16] highlights the importance and potential of cytotoxic agents that act through irreversible necrotic cell death.

B16 cells consistently demonstrated a higher resistance to TTO and terpinen-4-ol than AE17 cells as observed by MTT assay, but lower levels of cell death by apoptosis and necrosis induced indicated other potential mechanisms of action could be involved in their in vitro anticancer activity. Video time lapse microscopy showed untreated AE17 and B16 cells dividing at a normal rate compared to TTO-treated cells, particularly B16 cells, which displayed very low level cell division. This was confirmed as both TTO and terpinen-4-ol induced significant cell cycle arrest in both AE17 and B16 cell lines as assessed by flow cytometry. Specifically, significantly greater G1 cell cycle arrest

was observed in B16 cells when compared with AE17 cells with both TTO and terpinen-4-ol. Interestingly, cell phase arrest appeared to be time-dependent. Staurosporine included as a positive control, arrested both cell lines in G1 phase, which is consistent with the arrest in G1 of breast carcinoma cells following the same concentration of staurosporine [45]. The observation that both TTO and terpinen-4-ol can induce cancer cell cycle arrest has not previously been reported in the literature; moreover, it is a feature of promising anticancer terpenes and clinical chemotherapeutic agents. POH induced a G1 arrest in A549 lung cancer cells [6, 7] and a G2/M arrest in PC3 prostate cancer cells [46], whilst ingenol 3-angelate arrested Colo205 colon cancer cells in G1 phase following treatment [47]. G2/M arrest is evident following treatment with clinical agents, paclitaxel [48] and cisplatin [49], and both can also blockade cells in G1 phase [50].

In summary, we have shown doses of TTO and its major component terpinen-4-ol to have significant anti-proliferative activity against two tumour cell lines at doses non-cytotoxic in non-tumour fibroblast cells. Both TTO and terpinen-4-ol induce AE17 and B16 cell death by primary necrosis, low level apoptosis, and for the first time we have demonstrated TTO and terpinen-4-ol induce cell cycle arrest. These observations that TTO and terpinen-4-ol not only induced cell death, but also inhibited the growth of these aggressive tumour cells highlights the potential anticancer activity of TTO and terpinen-4-ol. Further studies to elucidate the molecular mechanisms of necrotic cell death and cell cycle arrest in these and other cancer cell lines, coupled with characterisation of possible efficacy in vivo are currently underway.

Acknowledgments This work was supported by a grant (PRJ-002395) from the Rural Industries Research and Development Corporation ACT, Australia and Novasel Australia Pty. Ltd., Mudgeeraba, QLD, Australia. We acknowledge the facilities, scientific and technical assistance of the Australian Microscopy & Microanalysis Research Facility at the Centre for Microscopy, Characterisation & Analysis (CMCA), The University of Western, Australia, a facility funded by The University, State and Commonwealth Governments and in particular Dr Paul Rigby (CMCA) for his help with the video time lapse microscopy. We would like to thank Pierre Filion and Robert Cook from the Electron Microscopy Unit at PathWest Laboratory Medicine WA for their technical advice, the use of reagents and equipment and helpful discussions.

References

1. Wagner KH, Elmadfa I (2003) Biological relevance of terpenoids. Overview focusing on mono-, di- and tetraterpenes. Ann Nutr Metab 47:95–106
2. Paduch R, Kandefer-Szerszen M, Trytek M, Fiedurek J (2007) Terpenes: substances useful in human healthcare. Arch Immunol Ther Exp (Warsz) 55:315–327
3. Gershenzon J, Dudareva N (2007) The function of terpene natural products in the natural world. Nat Chem Biol 3:408–414
4. Markman M, Mekhail TM (2002) Paclitaxel in cancer therapy. Expert Opin Pharmacother 3:755–766
5. Clark SS, Perman SM, Sahin MB, Jenkins GJ, Elegbede JA (2002) Antileukemia activity of perillyl alcohol (POH): uncoupling apoptosis from G0/G1 arrest suggests that the primary effect of POH on Bcr/Abl-transformed cells is to induce growth arrest. Leukemia 16:213–222
6. Yeruva L, Pierre KJ, Elegbede A, Wang RC, Carper SW (2007) Perillyl alcohol and perillic acid induced cell cycle arrest and apoptosis in non small cell lung cancer cells. Cancer Lett 257:216–226
7. Elegbede JA, Flores R, Wang RC (2003) Perillyl alcohol and perillaldehyde induced cell cycle arrest and cell death in BroTo and A549 cells cultured in vitro. Life Sci 73:2831–2840
8. Burke YD, Ayoubi AS, Werner SR, McFarland BC, Heilman DK, Ruggeri BA, Crowell PL (2002) Effects of the isoprenoids perillyl alcohol and farnesol on apoptosis biomarkers in pancreatic cancer chemoprevention. Anticancer Res 22:3127–3134
9. Stark MJ, Burke YD, McKinzie JH, Ayoubi AS, Crowell PL (1995) Chemotherapy of pancreatic cancer with the monoterpene perillyl alcohol. Cancer Lett 96:15–21
10. Da Fonseca CO, Masini M, Futuro D, Caetano R, Gattass CR, Quirico-Santos T (2006) Anaplastic oligodendroglioma responding favorably to intranasal delivery of perillyl alcohol: a case report and literature review. Surg Neurol 66:611–615
11. da Fonseca CO, Schwartsmann G, Fischer J, Nagel J, Futuro D, Quirico-Santos T, Gattass CR (2008) Preliminary results from a phase I/II study of perillyl alcohol intranasal administration in adults with recurrent malignant gliomas. Surg Neurol 70:259–266 discussion 266–267
12. Ogbourne SM, Suhrbier A, Jones B, Cozzi SJ, Boyle GM, Morris M, McAlpine D, Johns J, Scott TM, Sutherland KP, Gardner JM, Le TT, Lenarczyk A, Aylward JH, Parsons PG (2004) Antitumor activity of 3-ingenyl angelate: plasma membrane and mitochondrial disruption and necrotic cell death. Cancer Res 64:2833–2839
13. Hampson P, Chahal H, Khanim F, Hayden R, Mulder A, Assi LK, Bunce CM, Lord JM (2005) PEP005, a selective small-molecule activator of protein kinase C, has potent antileukemic activity mediated via the delta isoform of PKC. Blood 106:1362–1368
14. Hampson P, Kavanagh D, Smith E, Wang K, Lord JM, Ed Rainger G (2008) The anti-tumor agent, ingenol-3-angelate (PEP005), promotes the recruitment of cytotoxic neutrophils by activation of vascular endothelial cells in a PKC-delta dependent manner. Cancer Immunol Immunother 57:1241–1251
15. Cozzi SJ, Parsons PG, Ogbourne SM, Pedley J, Boyle GM (2006) Induction of senescence in diterpene ester-treated melanoma cells via protein kinase C-dependent hyperactivation of the mitogen-activated protein kinase pathway. Cancer Res 66:10083–10091
16. Siller G, Gebauer K, Katsamas J, Ogbourne SM (2009) PEP005 (ingenol mebutate) gel, a novel agent for the treatment of actinic keratosis: results of a randomized, double-blind, vehicle-controlled, multicentre, phase IIa study. Australas J Dermatol 50:16–22
17. Carson CF, Hammer KA, Riley TV (2006) *Melaleuca alternifolia* (tea tree) oil: a review of antimicrobial and other medicinal properties. Clin Microbiol Rev 19:50–62
18. Hammer KA, Carson CF, Riley TV (2003) Antifungal activity of the components of *Melaleuca alternifolia* (tea tree) oil. J Appl Microbiol 95:853–860
19. Schnitzler P, Schon K, Reichling J (2001) Antiviral activity of Australian tea tree oil and eucalyptus oil against herpes simplex virus in cell culture. Pharmazie 56:343–347
20. Hart PH, Brand C, Carson CF, Riley TV, Prager RH, Finlay-Jones JJ (2000) Terpinen-4-ol, the main component of the essential oil of *Melaleuca alternifolia* (tea tree oil), suppresses inflammatory mediator production by activated human monocytes. Inflamm Res 49:619–626

21. Mondello F, De Bernardis F, Girolamo A, Cassone A, Salvatore G (2006) In vivo activity of terpinen-4-ol, the main bioactive component of *Melaleuca alternifolia* Cheel (tea tree) oil against azole-susceptible and -resistant human pathogenic Candida species. BMC Infect Dis 6:158
22. Hayes AJL, Leach DN, Markham JL, Markovic B (1997) In vitro cytotoxicity of Australian tea tree oil using human cell lines. J Essent Oil Res 9:575–582
23. Calcabrini A, Stringaro A, Toccacieli L, Meschini S, Marra M, Colone M, Salvatore G, Mondello F, Arancia G, Molinari A (2004) Terpinen-4-ol, the main component of *Melaleuca alternifolia* (tea tree) oil inhibits the in vitro growth of human melanoma cells.[see comment]. J Invest Dermatol 122:349–360
24. Moteki H, Hibasami H, Yamada Y, Katsuzaki H, Imai K, Komiya T (2002) Specific induction of apoptosis by 1, 8-cineole in two human leukemia cell lines, but not a in human stomach cancer cell line. Oncol Rep 9:757–760
25. Jackaman C, Bundell CS, Kinnear BF, Smith AM, Filion P, van Hagen D, Robinson BW, Nelson DJ (2003) IL-2 intratumoral immunotherapy enhances CD8+ T cells that mediate destruction of tumor cells, tumor-associated vasculature: a novel mechanism for IL-2. J Immunol 171:5051–5063
26. Davis MR, Manning LS, Whitaker D, Garlepp MJ, Robinson BW (1992) Establishment of a murine model of malignant mesothelioma. Int J Cancer 52:881–886
27. Standardisation (2004) I.O.f., ISO 4730:2004: Oil of Melaleuca, Terpinen-4-ol type (Tea Tree Oil). International Organisation for Standardisation, Geneva Switzerland
28. Lazzaro AV (1983) Technical note: improved preparation of fine needle aspiration biopsies for transmission electron microscopy. Pathology 15:399–402
29. Gillespie SK, Zhang XD, Hersey P (2004) Ingenol 3-angelate induces dual modes of cell death and differentially regulates tumor necrosis factor-related apoptosis-inducing ligand-induced apoptosis in melanoma cells. Mol Cancer Ther 3:1651–1658
30. Barthelman M, Chen W, Gensler HL, Huang C, Dong Z, Bowden GT (1998) Inhibitory effects of perillyl alcohol on UVB-induced murine skin cancer and AP-1 transactivation. Cancer Res 58:711–716
31. Clark SS (2006) Perillyl alcohol induces c-Myc-dependent apoptosis in Bcr/Abl-transformed leukemia cells. Oncology 70:13–18
32. Lluria-Prevatt M, Morreale J, Gregus J, Alberts DS, Kaper F, Giaccia A, Powell MB (2002) Effects of perillyl alcohol on melanoma in the TPras mouse model. Cancer Epidemiol Biomarkers Prev 11:573–579
33. Lu XG, Zhan LB, Feng BA, Qu MY, Yu LH, Xie JH (2004) Inhibition of growth and metastasis of human gastric cancer implanted in nude mice by d-limonene. World J Gastroenterol 10:2140–2144
34. Ji J, Zhang L, Wu YY, Zhu XY, Lv SQ, Sun XZ (2006) Induction of apoptosis by d-limonene is mediated by a caspase-dependent mitochondrial death pathway in human leukemia cells. Leuk Lymphoma 47:2617–2624
35. Hakim IA, Harris RB, Ritenbaugh C (2000) Citrus peel use is associated with reduced risk of squamous cell carcinoma of the skin. Nutr Cancer 37:161–168
36. Soderberg TA, Johansson A, Gref R (1996) Toxic effects of some conifer resin acids and tea tree oil on human epithelial and fibroblast cells. Toxicology 107:99–109
37. Swamy SM, Huat BT (2003) Intracellular glutathione depletion and reactive oxygen species generation are important in alpha-hederin-induced apoptosis of P388 cells. Mol Cell Biochem 245:127–139
38. Rooney S, Ryan MF (2005) Effects of alpha-hederin and thymoquinone, constituents of *Nigella sativa*, on human cancer cell lines. Anticancer Res 25:2199–2204
39. Grossman D, Altieri DC (2001) Drug resistance in melanoma: mechanisms, apoptosis, and new potential therapeutic targets. Cancer Metastasis Rev 20:3–11
40. Fennell DA, Rudd RM (2004) Defective core-apoptosis signalling in diffuse malignant pleural mesothelioma: opportunities for effective drug development. Lancet Oncol 5:354–362
41. Mansour M, Pohajdak B, Kast WM, Fuentes-Ortega A, Korets-Smith E, Weir GM, Brown RG, Daftarian P (2007) Therapy of established B16–F10 melanoma tumors by a single vaccination of CTL/T helper peptides in VacciMax. J Transl Med 5:20
42. Ortega A, Ferrer P, Carretero J, Obrador E, Asensi M, Pellicer JA, Estrela JM (2003) Down-regulation of glutathione and Bcl-2 synthesis in mouse B16 melanoma cells avoids their survival during interaction with the vascular endothelium. J Biol Chem 278:39591–39599
43. Tang HL, Yuen KL, Tang HM, Fung MC (2008) Reversibility of apoptosis in cancer cells. Br J Cancer 100:118–122
44. Challacombe JM, Suhrbier A, Parsons PG, Jones B, Hampson P, Kavanagh D, Rainger GE, Morris M, Lord JM, Le TT, Hoang-Le D, Ogbourne SM (2006) Neutrophils are a key component of the antitumor efficacy of topical chemotherapy with ingenol-3-angelate. J Immunol 177:8123–8132
45. Kwon TK, Buchholz MA, Chrest FJ, Nordin AA (1996) Staurosporine-induced G1 arrest is associated with the induction and accumulation of cyclin-dependent kinase inhibitors. Cell Growth Differ 7:1305–1313
46. Rajesh D, Howard SP (2003) Perillyl alcohol mediated radiosensitization via augmentation of the Fas pathway in prostate cancer cells. Prostate. 57:14–23
47. Benhadji KA, Serova M, Ghoul A, Cvitkovic E, Le Tourneau C, Ogbourne SM, Lokiec F, Calvo F, Hammel P, Faivre S, Raymond E (2008) Antiproliferative activity of PEP005, a novel ingenol angelate that modulates PKC functions, alone and in combination with cytotoxic agents in human colon cancer cells. Br J Cancer 99:1808–1815
48. Wang T-H, Wang H-S, Soong Y-K (2000) Paclitaxel-induced cell death. Cancer 88:2619–2628
49. Sorenson CM, Barry MA, Eastman A (1990) Analysis of events associated with cell cycle arrest at G2 phase and cell death induced by cisplatin. J Natl Cancer Inst 82:749–755
50. Gibb RK, Taylor DD, Wan T, O'Connor DM, Doering DL, Gerçel-Taylor Ç (1997) Apoptosis as a measure of chemosensitivity to cisplatin and taxol therapy in ovarian cancer cell lines. Gynecol Oncol 65:13–22